Electronic Supplementary Information (ESI†)

Soluble inorganic quantum dots as electrolyte additives to boost lithium-sulfur battery performance

Liwei Liu, Ziyao Song, Zhihao Qi, Lijun Yang, Xizhang Wang, Zheng Hu* and Qiang Wu**

Key Laboratory of Mesoscopic Chemistry of MOE and Jiangsu Provincial Laboratory for Nanotechnology, School of Chemistry and Chemical Engineering, Nanjing University, Nanjing 210023, China

E-mail: wqchem@nju.edu.cn (Q. Wu); wangxzh@nju.edu.cn (X. Wang); zhenghu@nju.edu.cn (Z. Hu)

Experimental Section

Materials synthesis

The synthesis of MoS_2 QDs refers to the methods in the literature.[1, 2] The bulk MoS_2 powder was first stripped into nanosheets by solvent stripping method; typically, 1 g MoS_2 powder and 100 mL N-Methylpyrrolidone (NMP) were added into a 250 mL beaker, and then left for 12 h after ultrasound treatment. Then 2/3 of the upper liquid was poured into a flask and stirred vigorously at 140 °C for 6 h. The resulting suspension was centrifuged at 8000 rpm for 5 minutes, and the resulting light-yellow supernatant is MoS_2 QDs. The supernatant was frozen and dried to remove excess liquid, and the obtained solid powder is MoS_2 QDs powder.

As the cathode material, S/CNTs was synthesized by melt-diffusion method. The sulfur powder was mixed and ground with CNTs at a mass ratio of 7:3, and then the sealed mixture was heat treated at 155 °C under argon for 12 hours.

Visualization experiment

An appropriate amount of Li_2S and S (molar ratio 1:5) was added to the DOL/DME mixture, stirred at 55 °C overnight, and then diluted to produce Li_2S_6 solution (5 mmol L^{-1}). The MoS_2 QDs were dispersed in the DOL/DME electrolyte composed of 1 mol L^{-1} lithium bis(trifluoromethanesulfonyl)imide (LiTFSI) and 2 wt% $LiNO_3$ to obtain a solution with 0.1 wt % MoS_2 QDs. Then the Li_2S_6 solution was carefully added into the LSBs electrolyte or the

electrolyte with 0.1 wt% MoS_2 QDs, respectively. After standing for 1 h, the solution was vigorously shaken and the bottom solid was taken for the XPS analysis.

Characterization of electrocatalysis

The electrocatalytic function of the MoS_2 QDs was investigated by CV tests of symmetric cells or the dissolution and precipitation behaviors of Li_2S in asymmetric cells. To assemble a symmetrical battery, MoS_2 QDs were coated on a carbon paper (CP) disk (10.0 mm in diameter) with an average loading of 0.45 mg cm^{-2}. The 2032-type coin cell was then assembled using two CP disks, Celgard 2500 separator, and 40 μL DOL/DME electrolyte containing Li_2S_6 (2.5 mol L^{-1} for sulfur) and 1 mol L^{-1} LiTFSI. CV was tested at a scan rate of 3 mV s^{-1} on the VMP3 electrochemical workstation (Bio-logic), and charge transfer kinetics were studied by EIS (sinusoidal voltage amplitude 10 mV, frequency range 100 kHz~10 mHz). The experiment to measure the dissolution and precipitation behavior of Li_2S with and without MoS_2 QDs is conducted as follows: CP electrodes, lithium foil, Celgard 2500 separator, cathode electrolyte composed of 20 μL tetraglyme (containing 0.5 mol L^{-1} LiTFSI and 0.15 mol L^{-1} $LiNO_3$) dissolved with Li_2S_8 (2.5 mol L^{-1} for sulfur), 20 μL anode electrolyte (except that it does not contain Li_2S_8, which is same as the cathode electrolyte) is assembled into a 2032-type coin cell. First, a current of 0.10 mA was run to 1.80 V, followed by a constant current discharge at 0.01 mA to completely convert S to solid Li_2S. After that, the battery was charged at a constant potential at 2.40 V to dissolve the Li_2S until the charging current was below 0.01 mA. For nucleation and growth of Li_2S, maintaining a current of 0.112 mA discharged the battery to 2.06 V to reduce the higher-order polysulfides to Li_2S_4, and then maintaining a current of 2.05 V to below 0.01 mA. The electrocatalytic activity of different main materials was compared by the peak area of Li_2S dissolution and nucleation.

LSBs assembly and electrochemical tests

S/CNTs, acetylene black (AB), and polyvinylidene fluoride (PVDF) were added to the NMP at a mass ratio of 7:2:1 and stirred to form a uniform slurry. The slurry was coated on the CP plate and dried at 60 ℃ for 24 hours to make the working electrodes. Using working electrode, lithium foil, Celgard 2500 separator, electrolyte (the DOL/DME solution mixed with volume ratio 1:1, containing 1 mol L^{-1} LiTFSI, 2 wt% $LiNO_3$) with an E/S ratio of 20 μL mg^{-1} and the 2032-type coin cell, Li-S batteries were assembled. The MoS_2 QDs were dispersed in the above-mentioned electrolyte to assemble Li-S batteries in the same way. The Land CT2001 battery tester was used to test the charge and discharge performance of the batteries in the 1.7-2.8 V potential window. CV and EIS spectra were tested on a VMP3 electrochemical workstation. In addition, Li-S batteries with a high sulfur surface loading (~4 mg cm^{-2}) and a low E/S ratio (7 μL mg^{-1}) were assembled for performance evaluation.

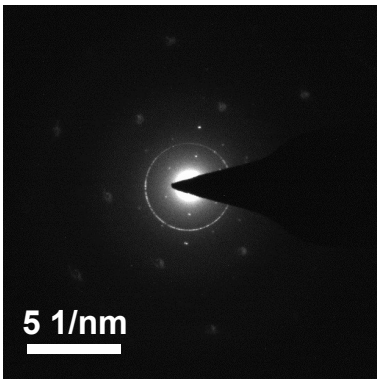

Fig. S1. Selected area electron diffraction (SAED) patterns of MoS_2 QDs.[1]

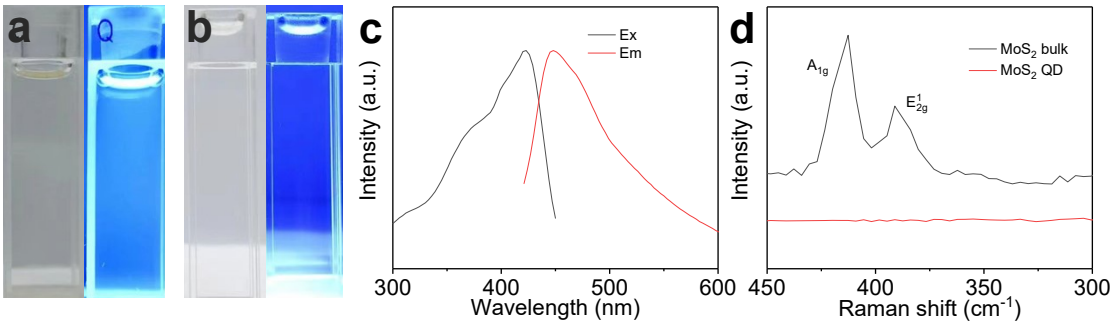

Fig. S2. (a) Photographs of MoS_2 QDs dispersed in ethanol without/with ultraviolet light irradiation. (b) Photographs of ethanol without/with ultraviolet light irradiation. (c) Excitation (Ex) and emission (Em) Photoluminescence (PL) spectra of MoS_2 QDs. (d) Raman spectra of MoS_2 bulk and MoS_2 QDs.

The fluorescence phenomenon was observed for the MoS_2 QDs-dispersed ethanol solution under the ultraviolet light irradiation, and the excitation and emission spectra have peaks at 420 nm and 450 nm, respectively, which further verifies the successful construction of MoS_2 QDs. Compared to MoS_2 bulk, MoS_2 QDs does not have peaks at A_{1g} and E1 2g, which may be caused by two factors: 1) residual solvents adsorbed on the quantum dots will weaken the Raman signal; 2) the lack of interlayer interactions can cause a sharp decrease in Raman intensity, indicating successful synthesis of MoS_2 QDs.[1]

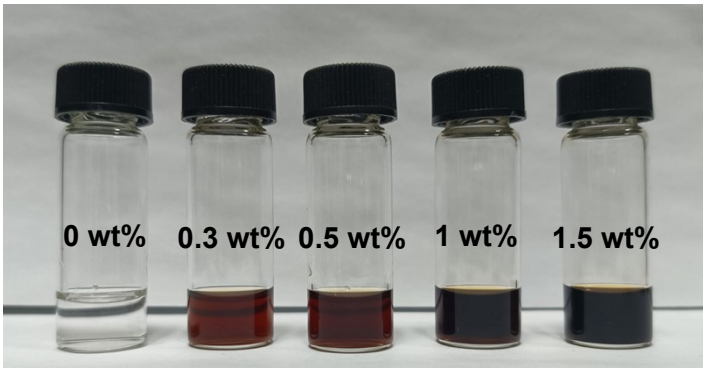

Fig. S3. Electrolytes with different MoS_2 QDs contents (0, 0.3, 0.5, 1.0, and 1.5 wt%). No insoluble powder was found at the bottom.

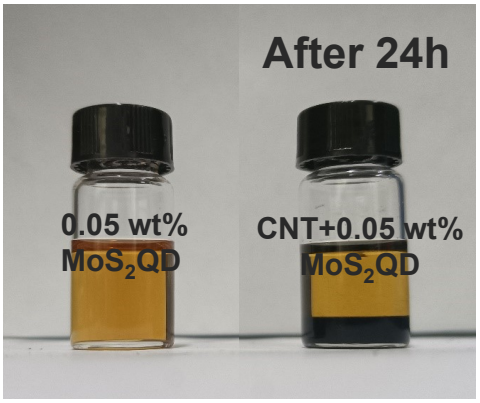

Fig. S4. 0.05 wt% MoS_2 QDs solution before and after adding the CNTs.

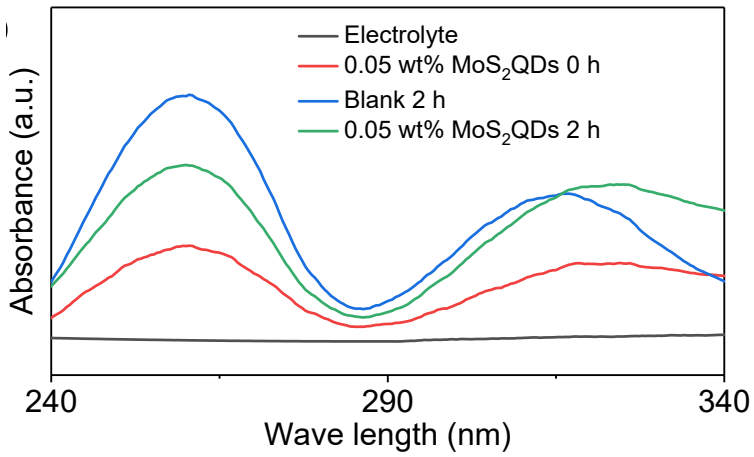

Fig. S5. UV-vis spectra of the electrolytes before and after 2 h of discharge. 0.05 wt% MoS_2 QDs 0 h and blank 2 h curve represent the UV-vis spectra of 0.05 wt% MoS_2 QDs and polysulfides in the electrolyte of Li-S batteries, respectively.

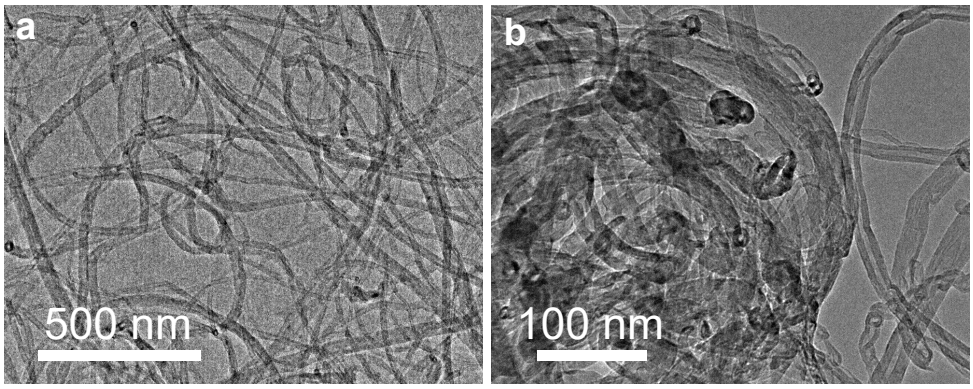

Fig. S6. TEM images of CNTs.

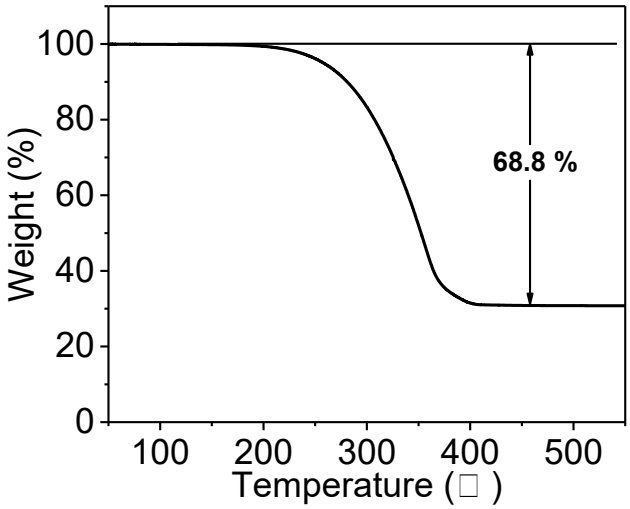

Fig. S7. Thermal gravimetric analysis (TGA) curve of S/CNTs.

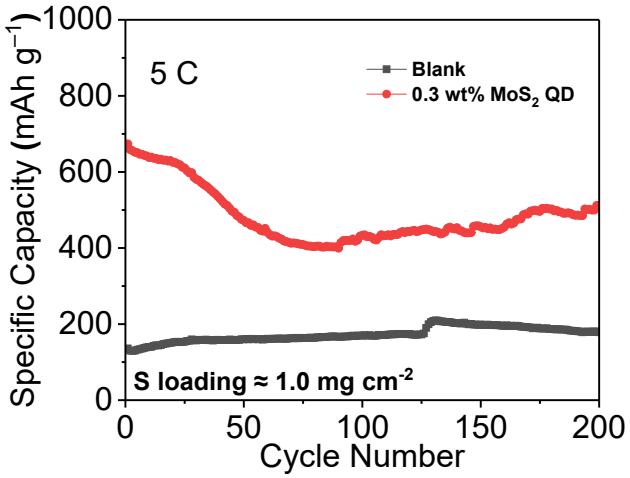

Fig. S8. Cycling performances at 5 C.

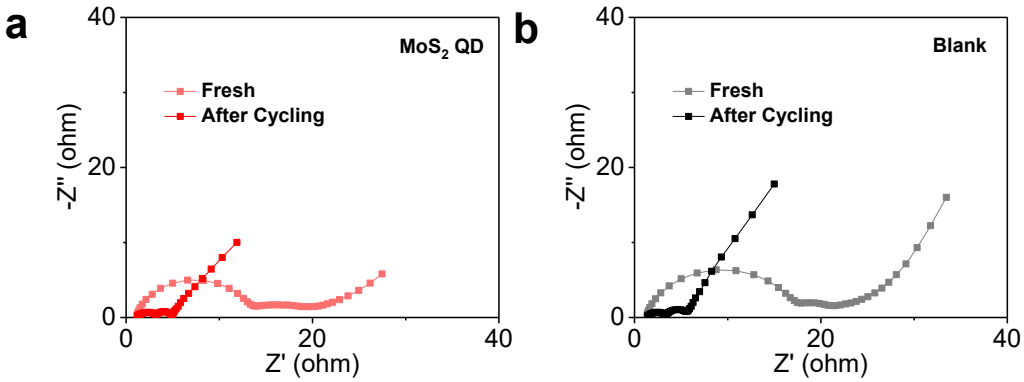

Fig. S9. EIS of LSBs with (a) and without (b) MoS_2 QDs before and after 50 cycles.

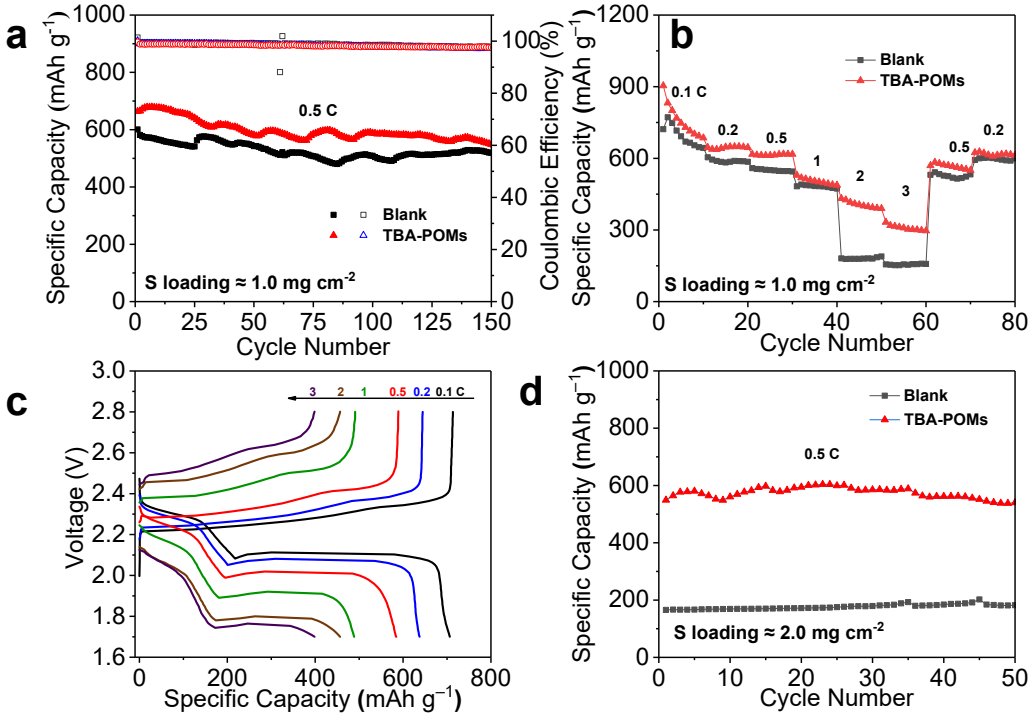

Fig. S10. Electrochemical performances of LSBs with or without TBA-POMs. (a) Cycling performances. (b) Rate performances. (c) Charge-discharge curves at different current density. (d) Cyclic performances with an areal S loading of ~2 mg cm^{-2}.

In order to verify the universality of this method, the soluble tetrabutylammonium polyoxometalates (TBA-POMs), i.e. $(TBA)_7[PW_{11}O_{39}]$, was used an electrolyte additive, and the current collector was replaced with Al foil.[3] As shown in Fig. S10a, the batteries with TBA-POMs exhibited better cycling performance. The battery with TBA-POMs can operate at 3C, while the counterpart without TBA-POMs cannot operate normally, indicating improved rate performance of Li-S batteries by adding TBA-POMs (Fig. S10b and c). With increased areal S loading, the LSB with TBA-POMs still exhibited better cycling performance (Fig. S10d). The results indicate that the TBA-POMs can improve the cycling and rate performances of Li-S batteries, indicating the universality of the strategy by using soluble QDs as electrolyte additives.

Table S1. Performances of Li-S batteries with various electrolyte additives

Sample	Current density (C)	Cycling number	Retention capacity (mAh g^{-1})	Rate capacity (mAh g^{-1}/C)	Reference
MoS_2 QDs	5	200	510	637/5	This study
Nitrogen-doped carbon dots	2	200	469	547/2	4
Di-t-butyl disulfide	4	150	312	566/4	5
Cobaltocene	2	100	552	/	6
Decamethylferrocene	0.1	150	490	/	7
5,7,12,14-pentacenetetrone	0.5	200	520	574/6	8

References

1. S. J. Xu, D. Li and P. Y. Wu, *Advanced Functional Materials*, 2015, **25**, 1127-1136.
2. H. H. Lin, C. X. Wang, J. P. Wu, Z. Z. Xu, Y. J. Huang and C. Zhang, *New Journal of Chemistry*, 2015, **39**, 8492-8497.
3. Z. Q. Li, L. W. Liu, C. H. Mao, C. K. Zhou, M. Q. Xia, Z. Shen, Y. Guo, Q. Wu, X. Z. Wang, L. J. Yang and Z. Hu, *Acta Chimica Sinica*, 2023, **81**, 620-626.
4. Y. Fu, Z. Wu, Y. Yuan, P. Chen, L. Yu, L. Yuan, Q. Han, Y. Lan, W. Bai, E. Kan, C. Huang, X. Ouyang, X. Wang, J. Zhu and J. Lu, *Nature Communications*, 2020, **11**, 845.
5. M. Zhao, B.-Q. Li, X. Chen, J. Xie, H. Yuan and J.-Q. Huang, *Chem*, 2020, **6**, 3297-3311.
6. M. Zhao, H.-J. Peng, J.-Y. Wei, J.-Q. Huang, B.-Q. Li, H. Yuan and Q. Zhang, *Small Methods*, 2020, **4**, 1900344.
7. S. Meini, R. Elazari, A. Rosenman, A. Garsuch and D. Aurbach, *The Journal of Physical Chemistry Letters*, 2014, **5**, 915-918.
8. Y.-Q. Peng, M. Zhao, Z.-X. Chen, Q. Cheng, Y. Liu, X.-Y. Li, Y.-W. Song, B.-Q. Li and J.-Q. Huang, *Nano Research*, 2023, **16**, 8253-8259.